Control of Vibration of Transmission Lines

Marcel Migdalovici, Tudor Sireteanu and Emil M. Videa

Institute of Solid Mechanics, Romanian Academy, Bucharest, Romania

(Revised 22 October 2009; accepted 27 January 2010)

The problem of vibration control of overhead line conductors subjected to laminar transverse wind, which induces stationary vibrations by Kármán effect, is important due to the consequences on these structures lifetime and service. We consider the conductor (cable) model as the Euler-Bernoulli beam, fulfilling the authors' condition that detaches the conductor model of the beam model with viscous, hysteretic, or dry friction internal-damping hypothesis. The aeolian vibration control of the conductor is based on the energy-balance principle that takes accounts for the wind-energy input, the energy dissipated by the conductor due to hysteretic self-damping properties (or equivalent viscous damping) and, eventually, the energy dissipated by the Stockbridge dampers. The aim of this approach is to mitigate the vibration level of overhead line conductors. The original analytical expression of the free-vibration modes and the resonance-frequencies equation for the cable with clamped extremities have been produced. The analytical expression of the kinetic energy of the cable is compared with the amount of dissipated energy, obtained by experimental means, for the control of vibration of transmission lines. Some applications are presented here.

1. INTRODUCTION

We consider the cable model derived from the Euler-Bernoulli beam with viscous, hysteretic, or Coulomb internal damping.[1–11] The analytical expression of the free-vibration modes and the resonance-frequencies equation for the cable with clamped extremities are produced using our hypothesis of the cable imposed to the Euler-Bernoulli beam, essentially for accurate identification of the cable-model parameters. Highlighted in this paper is the property of any Euler-Bernoulli beam model to be substituted with our cable model for sufficient high frequencies because our hypothesis of the cable is respected by the Euler-Bernoulli beam in these conditions. The classic analytical solutions of the Euler-Bernoulli beam equation are applicable for low frequencies, but for high frequencies (see the case of fuel bundle beams of the nuclear power plant), our cable model gives analytical solutions. We were able to find some recent studies in our domain of interest.[12–21] Our experimental research was performed on a specialized stand endowed with an overhead conductor with clamped extremities, alone or with a choice of Stockbridge dampers, and mounted on the extreme zones of the span. The resonance frequencies and vibration modes of the conductor in the stand are also identified theoretically and experimentally. The possibility of analyzing the influence of the concentrated harmonic force, applied on the cable middle span, and the influence of the aeolian forces through their energy diagrams were discovered. This gives the possibility of using the energy-balance principle to determine the vibration level of the cable at the resonance and the dynamic bending strain of the cable, versus frequencies, in the domain of interest. The analytical aspects of the internal-damping terms influence versus frequencies in the cable models are discussed.

2. MATHEMATICAL MODEL OF CABLE WITH GENERAL DAMPING

The following equation of free vibrations is considered:[1–7]

$$m_L \frac{\partial^2 w_i}{\partial t^2} = - c_i^{H*} w_i - \left(c_i^V + \frac{c_i^H}{\omega_i^{VH}} \right) \frac{\partial w_i}{\partial t} + \\ + T \frac{\partial^2 w_i}{\partial x^2} - EI \frac{\partial^4 w_i}{\partial x^4} + q. \quad (1)$$

Equation (1) describes the behavior of the cable, excited by the force $q = q(x,t)$, applied transversal on the cable, acting in the point of abscissa x at time t, on the viscous damping hypothesis by the constant coefficient c_i^V, on the hysteretic damping hypothesis by the constant coefficient of the form c_i^H/ω_i^{VH}, and on the dry friction (Coulomb) damping hypothesis, expressed by the coefficient c_i^{H*}. The coefficient c_i^{H*} is, piecewise, constant, as a function of time t, and the sign is such that the sign of the damping force $c_i^{H*} w_i(x,t)$ is opposite to that of the velocity $\dot{w}_i(x,t) = \partial w_i(x,t)/\partial t$ at any time t. Other explicit expression of the dry-friction force is $c_i^{H1} |w_i(x,t)| sign(\dot{w}_i(x,t))$, where c_i^{H1} is constant.[7] The first expression of the dry-friction force is deduced, in our case, taking into account that the functions $w_i(x,t)$ and $\partial w_i(x,t)/\partial t$ continue with separable variables. We denote by ω_i^{VH} the circular frequency of order i for damped free vibration, by $f_i^{VH} = \omega_i^{VH}/\pi/2$ the resonance frequency of order i for damped free vibration, by m_L the mass unit length of the cable, by EI the bending rigidity of the cable, by T the tension in the cable, by $y_i(x,t)$ the corresponding vertical displacement of the cable for vibration mode of order i, and by L the span length of the cable.

Firstly, we searched the stabilized free transverse vibrations of the cable without damping and with clamped extremities, which are of standing waves form:

$$w_r(x,t) = w_r(x) sin(\omega_r t + \varphi). \quad (2)$$

In Eq. (2), the notations signify that $\omega_r = 2\pi f_r$ is the circular frequency, with f_r the resonance frequency of the cable in free vibrations without damping, and that φ is the phase angle between the initial impulse and displacement. The following

dimensionless notations appear below:[3]

$$\alpha^2 = \frac{TL^2}{EI},\ \delta_r = \left[\frac{\alpha^2}{2} + \left(\frac{\alpha^4}{4} + \beta_r^4\right)^{\frac{1}{2}}\right]^{\frac{1}{2}},$$

$$\beta_r^4 = \frac{m_L\omega_r^2 L^4}{EI},\ \varepsilon_r = \left[-\frac{\alpha^2}{2} + \left(\frac{\alpha^4}{4} + \beta_r^4\right)^{\frac{1}{2}}\right]^{\frac{1}{2}}.$$

The expressions α, β_r, δ_r, ε_r verify the relationships:

$$\delta_r^2 - \varepsilon_r^2 = \alpha^2,\ \delta_r\varepsilon_r = \beta_r^2,$$
$$\delta_r^4 - \alpha^2\delta_r^2 - \beta_r^4 = 0,\ \varepsilon_r^4 + \alpha^2\varepsilon_r^2 - \beta_r^4 = 0. \quad (3)$$

We searched for the solution of Eq. (1) using the condition performed by the cable wire in the cases studied in the literature, which represents our hypothesis that detaches the cable model of the beam model:[8–11]

$$e^{-\delta_r} \approx 0. \quad (4)$$

For the clamped cable, the equation of resonance frequencies is[8–11]

$$\alpha^2 sin\varepsilon_r - 2\beta_r^2 cos\varepsilon_r = 0. \quad (5)$$

The analytical expression of the free vibration modes for undamped free vibrations of the cable in the case of clamped boundary conditions is shown in (6):

$$w_r(x) = C_r\left\{e^{-\delta_r\xi} + \frac{\delta_r}{\varepsilon_r}sin\varepsilon_r\xi - cos\varepsilon_r\xi + \right.$$
$$\left. -\frac{\delta_r}{\varepsilon_r}e^{\delta_r(\xi-1)}sin\varepsilon_r + e^{\delta_r(\xi-1)}cos\varepsilon_r\right\},\ \xi = \frac{x}{L}. \quad (6)$$

The factor C_r for each $r = 1, 2, \ldots$ is a constant. Anyone can verify that any Euler-Bernoulli beam model can be substituted with our cable model for sufficient high frequencies because $\delta_r \underset{r}{\longrightarrow} \infty$ and, thus, $e^{-\delta_r} \underset{r}{\longrightarrow} 0$.

We specify the following particular solutions $w_r(x)$ of the cable model that defines Eq. (2) in the case $q(x,t) = 0$, $c_r^V = 0$, $c_r^H = 0$, $c_r^{H*} = 0$, that also define the particular solutions of the beam model:

$$w_{1r}(x) = e^{-\delta_r\xi},\ w_{2r}(x) = e^{\delta_r\xi},$$
$$w_{3r}(x) = sin\varepsilon_r\xi,\ w_{4r}(x) = cos\varepsilon_r\xi,\ \xi = \frac{x}{L}. \quad (7)$$

The relations from Eq. (3) can be used to justify the particular solutions in Eq. (7).

The vibration mode of undamped vibration, expressed by relations Eqs. (2) and (6), is a solution of Eq. (1), where $q(x,t) = 0$, $c_i^V = 0$, $c_i^H = 0$, $c_i^{H*} = 0$ because $w_r(x)$ from Eq. (6) is a linear expression of the particular solutions from Eq. (7). The vibration mode of Eq. (2) also verifies the imposed boundary conditions.

In the case of the damped free vibrations described by Eq. (1), one searches for the solution of the form $w_i(x,t) = X_i(x)T_i(t)$, where $X_i(x)$ defines a vibrating mode of order i from Eq. (6). The equation deduced from Eq. (1) for the unknown function $T_t(t)$ is as follows:

$$\frac{d^2T_i(t)}{dt^2} + 2c_i^{VH}\frac{dT_i(t)}{dt} + c_i^{\Omega H*}T_i(t) = 0,$$
$$c_i^{VH} = c_i^V/m_L/2 + c_i^H/m_L/\omega_i^{VH}/2,$$
$$c_i^{\Omega H*} = \omega_i^2 + c_i^{H*}/m_L, \quad (8)$$

Equation (8) is deduced using the relationship

$$EI\frac{d^4X_i(x)}{dx^4} - T\frac{d^2X_i(x)}{dx^2} = \omega_i^2 m_L X_i(x). \quad (9)$$

In Eq. (8), ω_i is the circular frequency of the free undamped vibration of the cable, and ω_i^{VH} is the circular frequency of the free damped vibration of the cable.

The characteristic equation attached to Eq. (8) is as follows:

$$Z_i^2 + 2c_i^{VH}Z_i + c_i^{\Omega H*} = 0, \quad (10)$$

The solutions of Eq. (10) are

$$Z_{i_1} = -c_i^{VH} + \left\{\left(c_i^{VH}\right)^2 - c_i^{\Omega H*}\right\}^{1/2},$$
$$Z_{i_2} = -c_i^{VH} - \left\{\left(c_i^{VH}\right)^2 - c_i^{\Omega H*}\right\}^{1/2}. \quad (11)$$

If $c_i^{\Omega H*} < \left(c_i^{VH}\right)^2$ such that $\omega_i^2 < \left(c_i^{VH}\right)^2 - c_i^{H*}/m_L$, then the general solution of Eq. (8) is

$$T_i(t) = C_1e^{Z_{i_1}t} + C_2e^{Z_{i_2}t}. \quad (12)$$

The solution (12) does not describe our physical model. It is necessary to take into account the inequality $\omega_i^2 \geq \left(c_i^{VH}\right)^2 - c_i^{H*}/m_L$ or $\omega_i^2 + c_i^{H*}/m_L \geq \left(c_i^{VH}\right)^2$.

In the above case, there exists the solution described below:

$$T_i(t) = e^{c_i^{VH}t}\left\{C_{1i}sin\omega_i^{VH}t + C_{2i}cos\omega_i^{VH}t\right\},$$
$$\omega_i^{VH} = \left\{\omega_i^2 + c_i^{H*}/m_L - \left(c_i^{VH}\right)^2\right\}^{\frac{1}{2}}, i = 1, 2, \ldots. \quad (13)$$

If the initial conditions for the searched solution of the form $w_i(x,t) = X_i(x)T_i(t)$ (with fixed index i) for Eq. (1) (where $q(x,t) = 0$) are chosen as $w_i(x_o,t_o) = D_{oi}$, $\frac{\partial w_i}{\partial t}(x_o,t_o) = V_{oi}$, where $X_i(x)$ is a vibrating mode defined by the formula in Eq. (6), then we consider the expression of the vibration mode as follows:

$$w_i(x,t) = \frac{X_i(x)}{X_i(x_o)}e^{-c_i^{VH}(t-t_o)}\left\{\left(c_i^{VH}\frac{D_{oi}}{\omega_i^{VH}} + \right.\right.$$
$$\left.\left. + \frac{V_{oi}}{\omega_i^{VH}}\right)sin\omega_i^{VH}(t-t_o) + D_{oi}cos\omega_i^{VH}(t-t_o)\right\}, \quad (14)$$

$$\omega_i^{VH} = \left\{\omega_i^2 + c_i^{H*}/m_L - \left(c_i^{VH}\right)^2\right\}^{\frac{1}{2}},\ i = 1, 2, \ldots.$$

From Eq. (14), for $t_o = 0$ and $v_o = 0$, we can write

$$w_i(x,t) = X_i(x)\frac{D_{oi}}{X_i(x_o)}e^{-c_i^{VH}t}\left\{\frac{c_i^{VH}}{\omega_i^{VH}}sin\omega_i^{VH}t + \right.$$
$$\left. + cos\omega_i^{VH}t\right\},\ i = 1, 2, \ldots. \quad (15)$$

The following notation and formulas are used in Eq. (15):

$$c_i^{VH}/\omega_i^{VH} = ctg(\alpha_i),\ \alpha_i = arcctg(c_i^{VH}/\omega_i^{VH}),$$
$$\alpha_i \in (0, \frac{\pi}{2}),\ sin^2(\alpha_i) = (\omega_i^{VH})^2/(\omega_i^2 + c_i^{H*}/m_L),$$
$$cos^2(\alpha_i) = (c_i^{VH})^2/(\omega_i^2 + c_i^{H*}/m_L). \quad (16)$$

Hence, the form deduced for the function $T_i(t)$ is

$$T_i(t) = D_i^{H*}e^{-c_i^{VH}t}sin(\omega_i^{VH}t + \alpha_i),\ i = 1, 2, \ldots,$$
$$D_i^{H*} = \frac{D_{oi}(\omega_i^2 + c_i^{H*}/m_L)^{1/2}}{X_i(x_o)\omega_i^{VH}}. \quad (17)$$

The function $\frac{dT_i(t)}{dt}$, deduced from Eq. (15), has the form:

$$\frac{dT_i(t)}{dt} = -D_i^{H*} e^{-c_i^{VH} t} sin(\omega_i^{VH} t),\ i = 1, 2, \ldots . \quad (18)$$

Between the parameters of the mathematical model of the cable, the following condition of compatibility arises for $i = 1, 2, \ldots$:

$$(\omega_i^{VH})^2 = \left\{ \omega_i^2 + \frac{c_i^{H*}}{m_L} - \left(\frac{c_i^V}{2m_L} + \frac{c_i^H}{2m_L \omega_i^{VH}} \right)^2 \right\}, \quad (19)$$

The condition of compatibility also has the following form:

$$4m_L^2 (\omega_i^{VH})^4 - \left(4m_L^2 + 4m_L c_i^{H*} + -(c_i^V)^2\right) (\omega_i^{VH})^2 + 2c_i^V c_i^H \omega_i^{VH} + (c_i^H)^2 = 0. \quad (20)$$

The infinite set of coefficients c_i^V, c_i^H, c_i^{H*}, $i = 1, 2, \ldots$ (with the possibility of repetition) is supposed to be bounded.

The formulas Eqs. (14) and (17) specify that the influence of the hysteretic and dry-friction damping are negligible for the vibration mode if this mode is high enough, since $c_i^{VH} \approx c_i^V / m_L / 2$, and $\omega_i^{VH} \approx \omega_i$ for sufficiently high frequencies. However, the influence of viscous damping is maintained. This property of the cable is confirmed experimentally as well.

Equation (14) can also be used for performing the objective function referred to unknown parameters EI, c_i^H, c_i^{H*}, c_i^V expressed theoretically and experimentally. We use cable displacements and the weighted least-square method to identify the specified parameters. The expression of the objective function is

$$f(EI, c_i^V, c_i^H, c_i^{H*}) = \sum_{i,x,t} w_i^{cof} \left\{ w_i^c(x,t) - w_i^{exp}(x,t) \right\}^2. \quad (21)$$

We use theoretical displacements $w_i^c(x,t)$ and experimental displacements $w_i^{exp}(x,t)$, theoretically calculated or experimentally measured in some points of abscises x, also for some moments of time and for some frequencies both in the domain of interest and where $w_i^{cof} = 1/(w_i^{exp}(x,t))^2$ assure the objective function is dimensionless.

To determine the parameters, we used the model of the cable defined by Eq. (1) on the hypothesis of viscous-free damping ($c_i^H = 0$, $c_i^{H*} = 0$) only. The parameters are the bending rigidity, EI, of the cable and the coefficient, c^V, of the viscous damping referred to in some frequencies in the domain of interest. The experimental values are measured by using an experimental stand with a single overhead cable. The span is $L = 32\,m$, the ends of the cable are well fixed, $T = 1333\,N$, and $m_L = 0.757\,kg/m$.

The analyzed frequencies, according to experimental values, are $f_9 = 11.89\,Hz$, $f_{15} = 19.5\,Hz$, and $f_{19} = 24.98\,Hz$. The points considered are $x_1 = 0.089\,m$, $x_2 = 2.0\,m$, and $x_3 = 16.2\,m$. The moments of time correspond to the main values of the displacements. The values of the bending rigidity, $EI\,(40\,Nm^2)$, and of viscous damping, $c^V\,(2.675\,Ns/m)$, are determined by the minimization of Eq. (21), which was adapted to this case.

The diagram of the damped displacement of the cable for the resonance frequency of $19.5\,Hz$, in the point of abscissa $x = 16.2\,m$ on the span of the overhead cable, is plotted in Fig. 1.

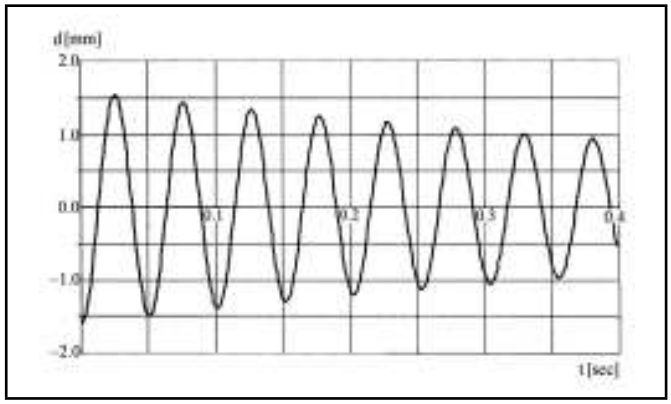

Figure 1. The diagram of damped displacement for resonance frequency.

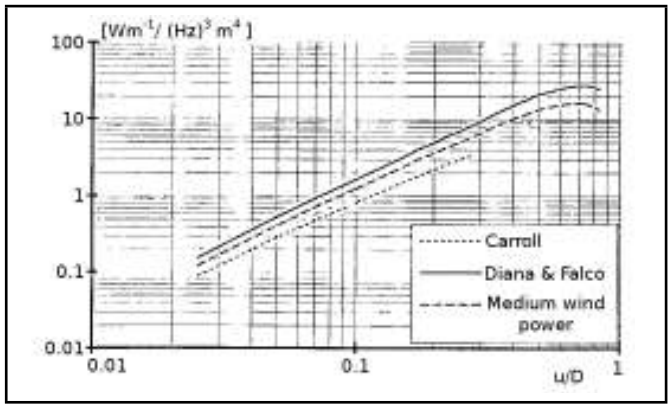

Figure 2. The empirical power induced by the wind.

3. THE ENERGY BALANCE PRINCIPLE

The energy balance principle is expressed by the following equation:[2]

$$E^w = E_C^d + E_D^d, \quad (22)$$

with E^W serving as the energy induced by the wind, E_C^d and E_D^d serving as the energy dissipated by the cable for any mode of vibration, respectively by the dampers, and mounted on the extremities zones of the transmission line span. The energy balance permits us to determine the amplitude of the vibration mode analyzed and the dynamic bending strain of the cable, which is the key factor in evaluating the dynamical stress/strain in the cable and, thus, the position regarding the fatigue damage. The dynamic bending strain ε_r^b of the cable, at the rigidly clamped extremities, can be expressed by the following empirical relationship:[21]

$$\varepsilon_r^b = k_\varepsilon d y_r(x_b). \quad (23)$$

In relation to Eq. (23), $x_b = 0.089\,m$, d is the diameter of outer strand of the cable, $y_r(x_b)$ is the bending amplitude for the mode r of the cable vibration, and k_ε is the empirical coefficient.

Concerning the wind energy, several authors have studied the wind energy imparted to the conductor (see Fig. 2).[22]

For example, the following relationships, Eqs. (24)–(26), are deduced experimentally or theoretically:

$$\frac{P^w}{f^3 D^4} = \frac{E^w}{f^2 D^4} = fnc(y_o/D) = 10^z. \quad (24)$$

In the above formula, P^w is the wind power on the unit length of the conductor, E^w is the wind energy on the unit

length of the conductor, f is the frequency, D is the conductor diameter, y_o is the antinodes amplitude, y_o/D is defined as dimensionless amplitude, $fnc(y_o/D)$ is a reduced power (or reduced energy) of the wind and could be taken into account by power z of the form $z = \sum_n a_n X^n$, $X = log_1 0(2y_o/D)$.

For the experimental diagram of the wind energy of Diana (Italy) we propose the following analytical expression of the reduced power, defined by $z = \sum_{n=0}^{9} a_n X^n$ and $X = log_1 0(2y_o/D)$ with values $a_0, \ldots, a_9$ done by

$$\begin{aligned} &a_0 = 1.26575,\ a_1 = 1.69387,\ a_2 = -1.08622,\\ &a_3 = -12.7859,\ a_4 = -34.620,\\ &a_5 = -43.7526,\ a_6 = -31.583,\ a_7 = -13.190,\\ &a_8 = -2.96931,\ a_9 = -0.27798. \end{aligned} \tag{25}$$

The energy dissipated by the conductor per cycle, in the hypothesis of hysteretic damping only, is given by the relation[2]

$$E_r^c = \frac{\pi}{16} c^H \times r^3 \times Y_r^{02}/L^2. \tag{26}$$

In Eq. (26), r is the modal number, c^H is the hysteretic damping coefficient that depends of the type of the conductor, Y_r^o is the cycle amplitude of the conductor, and L is the span length.

The last term of the energy-balance equation will be evaluated in terms of the per-cycle frequency characteristics of the dampers when the cycle amplitude is D_o. This way, the experimental data $\{E_i^d(D_o, f)\}_{i \in N}$ can be extrapolated from the assumption of linearity of the dynamic system of the damper, spaced at abscissa x_i^d, for the frequency f_r and amplitude Y_r^o. We use the relation[8]

$$E_i^d(Y_r^o, f_r) = E_i^d(D_o, f_r) \left(\frac{Y_r^o}{D_o}\right)^2 sin^2\left(\pi r \frac{x_i^d}{L}\right). \tag{27}$$

The balance-energy relationship yields a transcendental equation for Y_r^o from which the amplitude of the r^{th} vibration mode is obtained.

The dynamic bending strain at the clamped extremities can be evaluated according to the relationship in Eq. (23) for all resonance frequencies in the range of practical interest, such as $f_m in \leq f_r \leq f_m ax$ The values of $f_m in$ and $f_m ax$ are given by the minimum and maximum wind velocities that can induce aeolian vibration in the conductor. The corresponding interval for the modal numbers can also be obtained. The resulting ε_r is compared with the maximum allowable value ε_a.

Based on the semi-analytical model presented above, an algorithm and a computing program were made in order to obtain the diagrams of dynamic bending strain versus frequency.

To illustrate the method, a span of a single ACSR 54/19 conductor type, without dampers or equipped with two dampers of the same kind, equally spaced from the span clamped extremities, was considered.

Table 1. Parameters for computation

Conductor diameter D [m]	3.15×10^{-2}
Diameter of the outer strands d [m]	3.5×10^{-3}
Hysteretic damping constant c^H [Nm]	10,791
Mass of conductor unit length m_L [Kg/m]	1.982
Span length L [m]	400; 800
Dynamic bending rigidity EI [Nm^2]	23.35
Air density ρ [Kg/m^3]	1.25
Strouhal constant k_s	0.185
Coefficient for D.B.S. evaluation k_ε [m^{-2}]	390
Traction force along the conductor T [N]	40,050

Two construction types of Stockbridge dampers were considered: one with two resonance frequencies (Avb5) from the current production of a specialized manufacturer and one with five resonance frequencies (AvbT), a prototype developed in our institute.

The diagrams of the energy dissipated per cycle (*Nm*) versus frequency (*Hz*) obtained on a hydraulic shaker for $D_o = 25 \times 10^{-5}\ m$ are shown in Figs. 3 and 6.

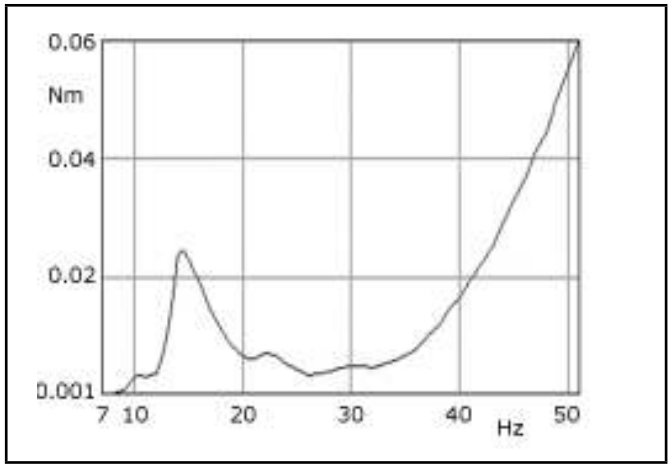

Figure 3. Energy dissipated by the Avb5 damper.

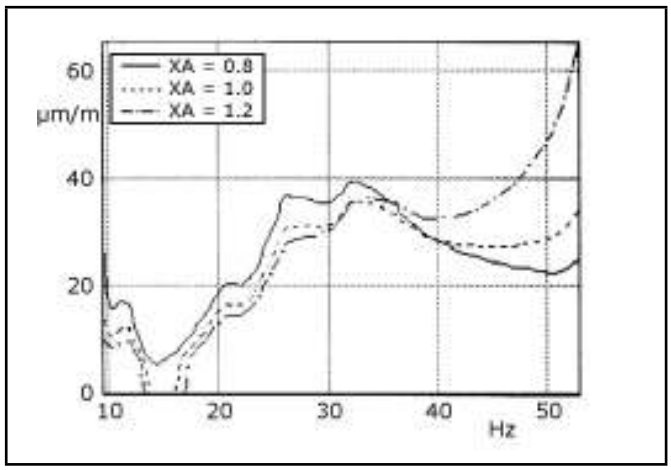

Figure 4. DBS for a conductor with Avb5 damper, L=400 m.

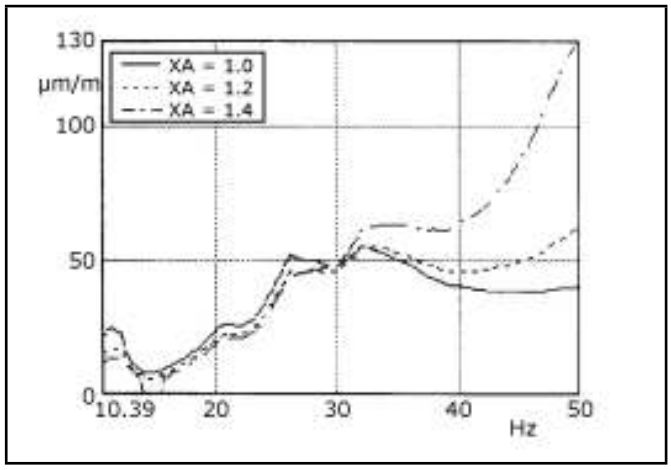

Figure 5. DBS. for a conductor with Avb5 damper, L=800 m.

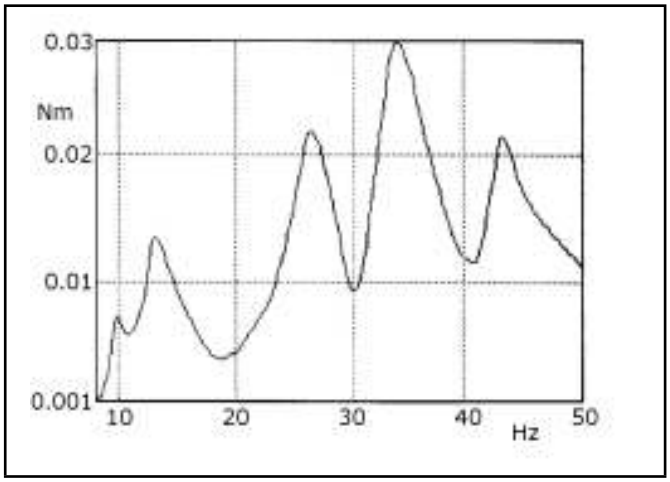

Figure 6. Energy dissipated by the AvbT damper.

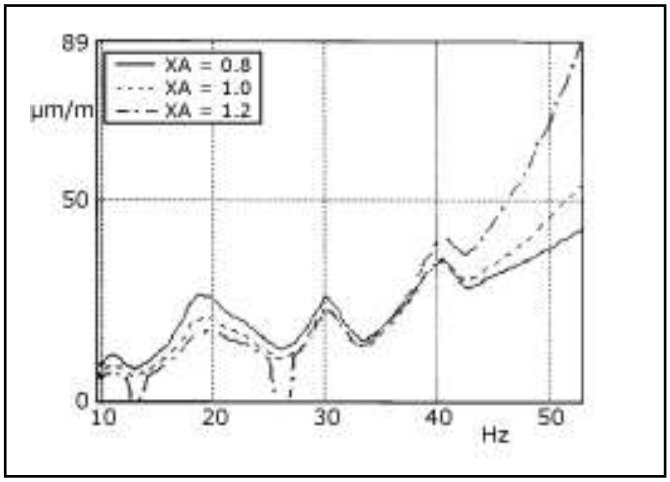

Figure 7. DBS for a conductor with AvbT damper, L=400 m.

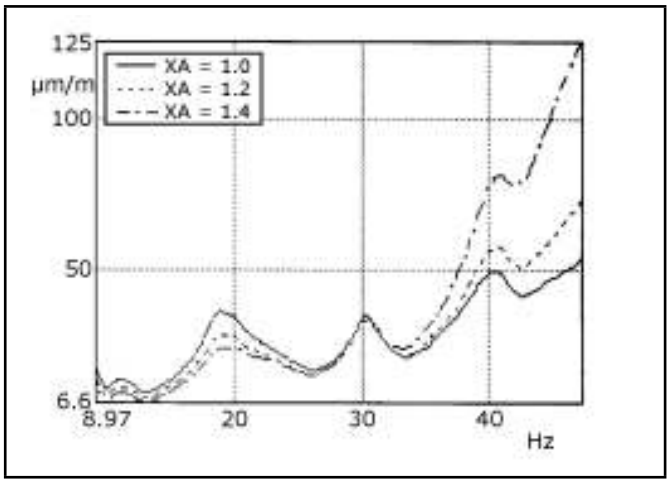

Figure 8. DBS for a conductor with AvbT damper, L=800 m.

The conductor tension T was chosen to represent 25% of its ultimate tensile stresses (UTS), which is the usual value for the conductor (EDS). The numerical values of the parameters used in the computations are given in Table 1. The numerical results are shown in Figs. 4, 5, 7, 8, as the diagrams of dynamic bending strain ($\mu m/m$) versus frequency (Hz) for different damper-spacing values denoted XA and measured in meters. The case of the span without dampers is obtained for $XA = 0$.

In the case studied, the dynamic bending strain (DBS) of the tested conductor is of small variability for all wind velocities that can induce aeolian vibration in the frequency range $10\,Hz$ – $50\,Hz$. This value is bigger than the maximum allowable bending strain. Therefore, the span must be provided with vibration dampers for both span extremity zones.

The effect of vibration dampers spaced in the usual range is obvious since the dynamic bending strain is in all cases reduced under the safety limit. The diagrams show that (AvbT) is more efficient then (Avb5), but both types could be used for the aeolian vibration control of the considered spans.

One can see that adequate damper spacing could further reduce the vibration level and implicit fatigue of the conductor. This spacing effect could become very important, especially when the dynamic bending strain was close to the maximum allowable value.

A comparison between a span of 400 m and a span of 800 m gives conclusions about the vibration level and the optimum position for dampers in each case. The model with analytical expression of the wind energy is more accurate than a model with concentrate wind force.

4. ANALYTICAL CONSIDERATIONS ON THE SYSTEM ENERGY

We considered the analytical expression in Eq. (14) of the solution $w_i(x,t) = X_i(x)T_i(t)$ (with fixed i) in the hypothesis of viscous damped free vibrations only for Eq. (1), with the values $q(x,t) = 0$, $c_i^H = 0$, $c_i^{H*} = 0$.

This solution is for a cable clamped to the extremities and with the initial conditions D_{oi}, V_{oi}. Also using the notations $\beta_{im} = c_i^V/m_L/2$ and $\omega_{i\beta}^2 = \omega_i^2 - \beta_{im}^2$, the kinetic energy per cycle of the cable, is

$$E_{ic} = \frac{1}{2} m_L \int_{t_o}^{t_o^\beta} \left(\frac{dT_i(t)}{dt}\right)^2 \left(\int_0^L X_i^2(x)dx\right) dt$$
$$t_0^\beta = t_0 + \frac{2\pi}{\omega_{i\beta}}. \tag{28}$$

The kinetic energy is evaluated using the values $x_0 = L/2$, $t_0 = 0$, and $V_{0i} = 0$. In this case, D_{oi} is the amplitude of the vibration mode.

Firstly, we calculate the integral referred to variable x. We deduce it as follows:

$$\int_0^L X_i^2(x)dx = L + L\left(\frac{3}{4\delta_i} + \frac{\alpha^2}{2\varepsilon_i^2} - \frac{5\delta_i}{4\varepsilon_i^2}\right) +$$
$$+ \frac{L}{\varepsilon_i}\left(\frac{\alpha^2}{4\varepsilon_i^2} + \frac{\alpha^2}{\delta_i^2+\varepsilon_i^2} + \frac{2\delta_i^2}{\delta_i^2+\varepsilon_i^2}\right) sin2\varepsilon_i +$$
$$+ L\left(\frac{\delta_i}{2\varepsilon_i^2} + \frac{\alpha^2\delta_i}{\varepsilon_i^2(\delta_i^2+\varepsilon_i^2)} - 2\frac{\delta_i}{\delta_i^2+\varepsilon_i^2} + \right.$$
$$\left. - \frac{\alpha^2}{4\delta_i\varepsilon_i^2}\right) cos2\varepsilon_i = Lk_L. \tag{29}$$

Also, we calculate

$$\int_{t_0}^{t_0^\beta} \left(\frac{dT_i(t)}{dt}\right)^2 dt = \frac{1}{x_{io}^2} \int_{t_0}^{t_0^\beta} e^{-2\beta_{im}^t} (VD_{oi})^2 dt,$$

$$t_0^\beta = t_0 + \frac{2\pi}{\omega_{i\beta}},\ \beta_{im}^t = \beta_{im}(t-t_0),\ X_{io}^2 = X_i^2(x_0),$$
$$VD_{oi} = V_{oi}cos\omega_{i\beta}^t - \omega_i^{DV} sin\omega_{i\beta}^t,$$
$$\omega_i^{DV} = \omega_i^2 \frac{D_{oi}}{\omega_{i\beta}} + \beta_{im}\frac{V_{oi}}{\omega_{i\beta}},\ \omega_{i\beta}^t = \omega_{i\beta}(t-t_0). \quad (30)$$

For $t_0 = 0$, $V_{oi} = 0$ we get

$$\int_0^{\frac{2\pi}{\omega_{i\beta}}} \left(\frac{dT_i(t)}{dt}\right)^2 dt = \frac{1 - e^{-4\pi\beta_{im}/\omega_{i\beta}}}{4X_i^2(x_0)\beta_{im}}\omega_i^2 D_{oi}^2,$$
$$\int_0^{\frac{2\pi}{\omega_{i\beta}}} \left(\frac{dT_i(t)}{dt}\right)^2 dt \approx \frac{\pi}{4X_i^2(x_0)\omega_{i\beta}}\omega_i^2 D_{oi}^2. \quad (31)$$

In the initial conditions for the damped free vibration $w_i(x,t)$, when D_{oi} is the ventral amplitude of the vibration mode, we can calculate the maximum kinetic energy (or power) and, therefore, the total energy of the cable, using these relations:

$$E_{ic} = \frac{1}{2}m_L \int_0^{\frac{2\pi}{\omega_{i\beta}}} \left(\frac{dT_i(t)}{dt}\right)^2 \left(\int_0^L X_i^2(x)dx\right) dt.$$
$$E_{ic} \approx \frac{\pi m_L L k_L}{2X_i^2(x_0)\omega_{i\beta}}\omega_i^2 D_{oi}^2 \quad (32)$$

$$X_i^2(x_0) = X_i^2(L/2) =$$
$$\frac{\delta_i^2 + \varepsilon_i^2}{2\varepsilon_i^2} - \frac{\alpha^2}{2\varepsilon_i^2}cos\varepsilon_i - \frac{\delta_i}{\varepsilon_i}sin\varepsilon_i. \quad (33)$$

The calculation of the kinetic energy of the cable can be compared with the percentage of the dissipated energy, obtained experimentally, from the total energy of the cable.

5. EXPERIMENTAL DEDUCTION OF THE DISSIPATED ENERGY

The experimental determination of the self-damping characteristic of a cable is based on the recommendations from specialty papers.[2,23–29]

For measuring the dissipated energy per cycle by a cable that vibrates in one of the free modes, there are several methods that can be grouped in two main categories: the methods of *free vibration* and *forced vibration*. The *forced vibration method* can be applied in two variants: the *stationary wave method* and the *power method*.

In the case of the *power method*, the one employed here, the conductor cable is excited to reach several possible resonances, and the induced power is directly determined by the product between the concentrated-force amplitude and the amplitude of the velocity of the resultant displacement, in the exciting point. In the stationary state, this power equals the self-dissipated power of the cable, with the condition that the two quantities are harmonic and in quadrate (a phase shift of $\pi/2$). Thus, the dissipated energy per cycle and, respectively, the power dissipated, have the same magnitude as the ones induced by the exciter. For such a regime, in the application point of excitation, one can write the following relations:

$$w = W_0 sin(2\pi ft - \theta_1),\ v = V_0 sin(2\pi ft - \theta_2),$$
$$F = F_0 sin(2\pi ft), \quad (34)$$
$$\theta_1 = \theta_1(f),\ \theta_2 = \theta_2(f), V_0 = 2\pi f W_0. \quad (35)$$

This method is faster and simpler than the other, but for good results it is necessary to minimize the losses of energy at the ends; therefore, one firmly embeds the cable in very solid clamps.

6. NUMERICAL RESULTS

A collective from our institute determined the self-damping of a conductor cable on an experimental site endowed with an Al-St 300/69 conductor, having the characteristics from Table 2:[26,28,29]

Table 2. Parameters of the conductor

Characteristic	Values	Dimension
Outer diameter	2.515×10^{-2}	m
Breaking force	129,603	N
Mass per unit length	1.389	Kg m^{-1}
Span length	28	m
traction	35000	N

First, one calculates the values of the total power of the cable at the resonance frequencies, using the relation (32), for the viscous internal-damping hypothesis ($c_i^H = 0$, $c_i^{H*} = 0$). Also, one experimentally performs the dissipated power of the cable (Fig. 9) and then calculates the percentage of the dissipated power from the total power induced to the cable. This percentage directly increases with the resonance frequency values.

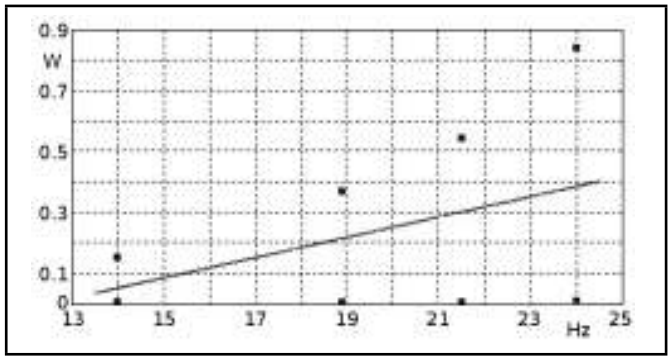

Figure 9. Experimentally dissipated power versus frequency.

7. CONCLUSIONS

The original analytical considerations about the definition of the cable in a viscous, hysteretic, or dry friction internal-damping hypothesis, using our cable model detached from the Euler-Bernoulli beam model, permit us to perform the analytical vibration modes of the cable and control these vibrations.

The energy-balance principle presented here can be used to establish the optimum values of the cable parameters such that the vibration level of the cable with or without Stockbridge dampers is in safety limits, taking into account the frequencies of the cable in the domain of interest.

From the last experimental results for the cable, we noticed that with the increase of the resonance frequencies value, the percentage of the dissipated power also increased, tending to reach almost 100% for higher frequencies, toward the limit of the common range. This proves that the self-damping is a very important component in the overall damping assessment.

We proved analytically that it is possible for the conductor cable to simultaneously consider the influence of viscous, hysteretic, and dry friction internal damping of the cable, but the hysteretic and dry-friction damping are negligible to maintain

a sufficiently high vibration mode of the cable while the influence of viscous damping is maintained.

The analytical results of the cable model are entered for the studies about how much can lead the analytical calculation in the mathematical modeling of the mechanical phenomena up to replacing with a numerical method of the solution calculation by using the numerical values of the parameters.[30] The large analytical phase for the deduction of the mathematical model of mechanical phenomena increases the precision of the results and shortens the time needed on the computer calculation.

REFERENCES

[1] Timoshenko, S. *Theorie des vibrations a l'usage des ingenieurs*, Librairie polytechnique Ch. Beranger, Paris et Liege, (1937).

[2] Claren, R., and Diana, G., Mathematical Analysis of Transmission Line Vibration, *IEEE Transactions*, **88**(12), 1741–1771, (1969).

[3] Nowacki, W., *The dynamics of the elastic systems*, Technical Publishing House, Bucharest, (1969). (in Romanian, translation from Polish)

[4] Chen, S. S., and Wambsganss, M. W., Parallel Flow-Induced Vibration of Fuel Rods, *Nuclear Engineering and Design*, **18**(2), 253–278, (1972).

[5] Thomson, W. T., *Theory of vibration with applications*, Allen & Unwin, Sydney, (1988).

[6] Poetsch, G., and all, Pantograph/ Catenary Dynamics and Control, *Vehicle System Dynamics*, **28**(2), 159–195, (1997).

[7] Guglielmino, E., Sireteanu, T., Stammers, C. W., Ghita, G., and Giuclea, M., *Semi-active Suspension Control*, Springer, London, (2008).

[8] Migdalovici, M., Sireteanu, T., and Videa, E., About the aeolian vibration control of overhead line conductors, Proceedings of the ASME-PVP Conference, San Diego, **366**, 119–122, (1998).

[9] Migdalovici, M., Onisoru, J., Videa, E., and Albrecht, Al. On the control of vibration of overhead line conductors, Proceedings of the ICSV11, St. Petersburg, 3589–3596, (2004).

[10] Migdalovici, M., Control of vibration of overhead line conductors, *Topics in applied mechanics*, Eds. Chiroiu, V., and Sireteanu, T. Romanian Academy Publishing House, Bucharest, 2004, **2**(8), 244–261.

[11] Migdalovici, M., and Baran, D., *Control of vibrations of some dynamical systems*, BREN Publishing House, Bucharest, (2006). (writen in Romanian)

[12] Behera, R. K., Parhi D. R. K., Sahu, S. K., Dynamic Characteristics of a Cantilever Beam with Transverse Cracks, *International Journal of Acoustics and Vibration*, **11**(1), 3–18, (2006).

[13] Mohanty, S. C., Parametric Instability of a Pretwisted Cantilever Beam with Localised Damage, *International Journal of Acoustics and Vibration*, **12**(4), 153–161, (2007).

[14] Das, H. C., and Parhi D. R., Damage Analysis of Cracked Structure Using Fuzzy Control Technique, *International Journal of Acoustics and Vibration*, **13**(2), 55–66, (2008).

[15] Georgakis, C. T., Taylor, C. A., Nonlinear dynamics of cable stays. Part I: sinusoidal cable support excitation, *Journal of Sound and Vibration*, **281**(3–5), 537–564, (2005).

[16] Firouz-Abadi, R. D., Haddadpour, H., and Novinzadeh, A. B., An asymptotic solution to transverse free vibrations of variable-section beams, *Journal of Sound and Vibration*, **304**(3–5), 530–540, (2007).

[17] Tanaka, N., and Iwamoto, H., Active boundary control of an Euler-Bernoulli beam for generating vibration-free state, *Journal of Sound and Vibration*, **304**(3–5), 570–586, (2007).

[18] Mikata, Y., Orthogonality condition for a multi-span beam, and its application to transient vibration of a two-span beam, *Journal of Sound and Vibration*, **314**(3–5), 851–866, (2008).

[19] Luongo, A., Zulli, D., Piccardo, G., Analytical and numerical approaches to nonlinear galloping of internally resonant suspended cables, *Journal of Sound and Vibration*, **315**(3–5), 375–393, (2008).

[20] Mazanoglu, K., Yesilyurt, I., Sabuncu, M., Vibration analysis of multiple-cracked non-uniform beams, *Journal of Sound and Vibration*, **320**(4–5), 977–989, (2009).

[21] Curami, A., and Beretta, A., Normative di collaudo di ammortizzatori di campata per linee aeree. Un confronto teorico e sperimentale, *L'Energia elettrica*, **778**, 325–334, (1991).

[22] CIGRE report W.G.01, S.C.22, Report on Aeolian Vibration, *Electra*, **124**, 41–77, (1989).

[23] Guide on self-damping measurements, *I.E.E.E.*, **563**, (1978).

[24] Agelink, G., CIGRE Report S 22-81, Results of overhead line conductor self-damping measurements, (1981).

[25] Rawlins, C. H., ALCOA Labs, Report No. 93-83-4, Notes on the measurements of conductor self-damping, (1983).

[26] Sireteanu, T., and Videa E. M., Contract IFTM — ICEMENERG, Self-damping characteristic determination for the cables Al–St, used to the overhead line conductors, (1988).

[27] CIGRE Report, SC22, WG11, TF1, Conductor self-damping, (1994).

[28] Videa, E. M., The electric analogy of the complex dynamic phenomena from the overhead electric cables excited by the wind and methods to mitigate the vibration level, PhD thesis, University Politehnica of Bucharest, (1995).

[29] Videa, E. M., *Research Trends in Mechanics*, Eds. Popa D., Chiroiu V., and Toma I., Romanian Academy Publishing House, Bucharest, **2**(15), 379–405, (2008).

[30] Migdalovici, M., On the Analytical and Numerical Computation in Mechanical Modeling, Proceedings of the European Computing Conference, Eds. Mastorakis, N., and Mladenov, V., Springer Science + Business Media, New York, **2**(7), 73–78, (2009).